Environmental Science and Pollution Research (2019) 26:775–783
https://doi.org/10.1007/s11356-018-3661-z

RESEARCH ARTICLE

The remediation potential and kinetics of cadmium in the green alga *Cladophora rupestris*

Hui-min Zhang[1] · Geng Geng[1] · Jun-jie Wang[1] · Yue Xin[1] · Qian Zhang[1] · De-ju Cao[1] · You-hua Ma[1]

Received: 5 August 2018 / Accepted: 1 November 2018 / Published online: 10 November 2018

Abstract

This study determined the subcellular distribution, chemical forms, and effects of metal homeostasis of excess Cd in *Cladophora rupestris*. Biosorption data were analyzed with Langmuir and Freundlich adsorption models and kinetic equations. Results showed that *C. rupestris* can accumulate Cd. Cd mainly localized in the cell wall and debris (42.8–68.2%) of *C. rupestris*, followed by the soluble fraction (22.1–38.4%) observed in *C. rupestris*. A large quantity of Cd ions existed as insoluble $CdHPO_4$ complexed with organic acids, $Cd(H_2PO_4)_2$, Cd-phosphate complexes (F_{HAC}) (43.2–56.0%), and pectate and protein-integrated Cd (F_{NaCl}) (30.8–43.2%). The adsorption data were well fitted by the Freundlich model ($R^2 = 0.933$) and could be described by the pseudo-second-order reaction rate ($R^2 = 0.997$) and Elovich ($R^2 = 0.972$) equations. Related parameters indicated that Cd adsorption by *C. rupestris* is a heterogeneous diffusion. Cd promoted Ca and Zn uptake by *C. rupestris*. Cu, Fe, Mn, and Mg adsorption was promoted by low Cd concentrations and inhibited by high Cd concentrations. Results suggested that cell wall sequestration, vacuolar compartmentalization, and chemical morphological transformation are important mechanisms of Cd stress tolerance by *C. rupestris*. This study suggests that *C. rupestris* has bioremediation potential of Cd.

Keywords Cd · *C. rupestris* · Kinetics · Bioaccumulation · Subcellular distribution · Chemical form

Introduction

Cadmium (Cd) is a nonessential element in macroalgae. It is highly mobile and toxic and can be enriched in animals and plants as it moves throughout the food chain. Cd can enter the human body when consumed and may cause kidney damage and cancer and impair lung function (Li et al. 2017; ATDR 2012). Therefore, the remediation of Cd pollution has become an important concern. Bioremediation is a promising technique for Cd remediation because of its eco-friendliness and cost-effectiveness (Zeraatkar et al. 2016). The green alga *Cladophora*, an important and ubiquitous component of freshwater environments, can be used for the phytoremediation of heavy metals (Cao et al. 2015a; Yang and Li 2015; Zeraatkar et al. 2016) and exists widely in natural water bodies of Anhui Province, China.

The subcellular distribution of heavy metals can provide information on the mechanism of heavy metal enrichment and tolerance (Hou et al. 2013). Cd exists in different chemical forms after assimilation by pokeweed (Fu et al. 2011). The toxicity and tolerance mechanisms for Cd are linked to its subcellular and chemical forms, greatly affecting its transport in plants (Meyer et al. 2015; Ma et al. 2015; Lavoie et al. 2009a). Similarly, the heavy metal tolerance and enrichment characteristics of hyperaccumulator plants are closely related to metal subcellular distribution and plant morphology (Lwalaba et al. 2017). Li et al. (2016) suggested that *Arbuscular mycorrhizal* fungi mainly enhance rice resistance to cadmium by altering the subcellular distribution and chemical forms of Cd. Mwamba et al. (2016) demonstrated that the difference between the subcellular distribution and chemical forms of Cd and Cu can improve the toxicity to *Brassica napus* plants. Therefore, investigating the subcellular and chemical forms of Cd in *Cladophora rupestris* is necessary to reveal the detoxification and absorption mechanisms of this alga.

Responsible editor: Elena Maestri

✉ De-ju Cao
cdj@ahau.edu.cn

You-hua Ma
yhma@ahau.edu.cn

[1] Anhui Province Key Laboratory of Farmland Ecological Conservation and Pollution Prevention, School of Resources and Environment, Anhui Agricultural University, Hefei 230036, People's Republic of China

Various absorption isotherms have been used to evaluate sorption characteristics (Kumar et al. 2016). A thermodynamic equation was used to determine the Cd biosorption capacity of living microalgae (Zhou et al. 2017). Xie et al. (2015) reported that the Freundlich model fitted biosorption data well and illustrated the complexation–biosorption properties of rice roots. Anastopoulos and Kyzas (2015) used isotherm models and kinetic equations to investigate the ability of algae to adsorb heavy metals and confirmed that micro- and macroalgae are promising biosorbents that can be used to remove heavy metals from wastewater. Cd^{2+} was affected on metal homeostasis in plants. The metal homeostasis of Fe, Mn, Ca, and Mg in *Camellia sinensis* was affected at Cd concentration of 1.0–15.0 mg/L (Cao et al. 2018).

The present investigation analyzed the subcellular distribution and chemical forms of Cd in *C. rupestris* under different levels of Cd stress. Langmuir and Freundlich, pseudo-first- and pseudo-second-order reaction, Elovich, and double-constant equations were used to analyze the Cd adsorption characteristics of *C. rupestris*. Moreover, the effects of Cd^{2+} on metal homeostasis in *C. rupestris* were analyzed. The findings of this study can provide references for the remediation of water polluted with heavy metals.

Materials and methods

Algae cultivation and preparation

Cladophora rupestris was collected from surface water of a pond in Hefei in Anhui Province, China (31°50′ N, 117°11′ E). The samples were grown in a sterilized medium at 25 °C and kept under an illumination intensity ranging from 3000 to 4000 lx (with a light:dark photoperiod of 12:12 h) in an incubator (SPX-250B-G). The cultures were kept at a pH of 7.0 ± 0.5 and grown without antibiotics (Cao et al. 2015a, 2015b).

Experimental design and *C. rupestris* cultivation

Three grams *C. rupestris* was exposed in 1000 mL BG11 medium (1.5 g $NaNO_3$, 40 mg $K_2HPO_4{\cdot}3H_2O$, 75 mg $MgSO_4{\cdot}7H_2O$, 36 mg $CaCl_2{\cdot}2H_2O$, 6 mg citric acid, 6 mg ferric ammonium citrate, 1 mg $Na_2EDTA{\cdot}2H_2O$, 20 mg Na_2CO_3, 2.86 mg H_3BO_3, 1.81 mg $MnCl_2{\cdot}4H_2O$, 0.22 mg $ZnSO_4{\cdot}7H_2O$, 0.39 mg $Na_2MoO_4{\cdot}2H_2O$, 0.079 mg $CuSO_4{\cdot}5H_2O$, and 0.0494 mg $CO(NO_3)_2{\cdot}6H_2O$ per liter) (Wang et al. 2017), and containing different concentrations of Cd (0.0, 0.5, 1.0, 2.5, 5.0, 7.5, or 10.0 mg/L) for 7 days. Cd (II) stock solutions (1000 mg/L) were prepared by dissolving $Cd(NO_3)_2$ in purified water. All solutions used in the experiments were obtained by means of stock solution dilution (Cao et al. 2015a). Each treatment was performed in three replicates.

Experiment and measurements

Before doing the subcellular fractionation and chemical form characterization of intracellular Cd, the carry-over Cd from the exposure solution and extracellular loosely bound Cd should be washed off from the algae samples with distilled water, and it is assumed not to affect cell physiology (Hassler et al. 2004; Lavoie et al. 2009b).

Subcellular partitioning procedure

After 7 days, the tissue fractionation of *C. rupestris* was on the basis of Cao et al. (2018): 1.0 g samples were frozen prior to the experiment. *Cladophora rupestris* tissues were homogenized in extraction buffer [50 mM HEPES, 1.0 mM DTT, 500 mM sucrose, 5.0 mM ascorbic acid, 1.0% (*w*/*v*) Polyclar ATPVPP, adjusted to pH 7.5]. Separation of subcellular fractions by differential centrifugation was the following process: the homogenate was centrifuged at 300×*g* for 30 s and the pellet was designated the cell wall fraction, consisting mainly of cell walls and cell wall debris (Lavoie et al. 2009a; Zhao et al. 2015). The filtrate was centrifuged at 20000×*g* for 45 min and the pellet designated as the organelle and the supernatant as the soluble fraction. The resultant pellets were resuspended in extraction buffer. All steps were performed at 4 °C.

Chemical form extraction

Following the method of Cao et al. (2018) and Zhao et al. (2015), frozen algal material (1.000 g) was mixed with 10 mL of extraction solution at 25 °C (24 h). The extraction solution was then separated, and the residual material was re-extracted with the same amount of extraction solution for 2 h. The twice-extracted solutions containing each chemical form of Cd were collected and separately wet digested. Different cadmium chemical forms were extracted successively by the following order: (1) 80% alcohol, extracting inorganic Cd, which included nitrate/nitrite, chloride, and aminophenol cadmium (F_E); (2) d-H_2O, extraction water-soluble fraction Cd of organic acid complexes and $Cd(H_2PO_4)_2$ (F_W); (3) 1MNaCl, extracting pectate and protein-integrated Cd (F_{NaCl}); (4) 2% HAC, extraction insoluble fraction $CdHPO_4$ with organic acids and $Cd(H_2PO_4)_2$ and other Cd-phosphate complexes (F_{HAC}); (5) 0.6 M HCl, extracting oxalate acid-bond Cd (F_{HCl}); and (6) Cd in the residue (F_R).

Determination of Cd and other element concentration

The samples were placed into 50-mL polytetrafluoroethylene tubes with 10 mL HNO_3 for 12 h under the fume hood and then heated on the graphite digestion apparatus at 105 °C for 1.5 h (ZEROM ProD40, Changsha Zerom Instrument and Meter Co., Ltd., China). Afterwards, 2 mL $HClO_4$ was added

and heated again at 135 °C for 30 min (Qiu et al. 2011; Cao et al. 2015a), and diluted with water to 50 mL. Cd concentrations in the digestion were determined by M5 Thermo flame atomic absorption spectrometry, operated at 228.8 nm with a hollow cathode lamp under an air/acetylene flame while the fuel gas flow rate was 40.0 L/h, and the slit width was 0.2 nm. The content of Ca, Zn, Mn, Fe, Mg, and Cu were analyzed by M5 flame atomic absorption spectrometry, used hollow cathode lamp as light source, and set the wavelength at 422.7 nm (Ca), 213.9 nm (Zn), 279.5 nm (Mn), 248.3 nm (Fe), 285.2 nm (Mg), and 324.7 nm (Cu) respectively.

Data analysis

Isotherm adsorption model

The Langmuir isotherm model assumes monolayer adsorption on a uniform surface with a finite number of adsorption sites and once a site is filled (Islam et al. 2015). The linear form is expressed as:

$$\frac{C_e}{Q_e} = \frac{1}{Q_{\max} b} + \frac{C_e}{Q_{\max}} \quad (1)$$

where Q_e is the amount of Cd(II) adsorbed per unit mass of *C. rupestris* at equilibrium (mg/g), C_e is the concentration of Cd(II) remaining in solution during adsorption equilibrium (mg/L), Q_{max} is Langmuir constant related to the maximum adsorption capacity (mg/g), and b is Langmuir constant related to free energy of adsorption (L/mg). The values of Q_{max} and b can be calculated from the slope and intercept of the $C_e / Q_e - C_e$.

The Freundlich isotherm model is an empirical equation based on non-ideal adsorption on a heterogeneous surface, describes the heterogeneity of the adsorbent surface or the interaction between the adsorbent surface and the adsorbate (Chakravarty and Banerjee 2012). The linear is expressed as:

$$\ln Q_e = \ln K_f + \frac{1}{n} \ln C_e \quad (2)$$

where Q_e is the amount of Cd(II) adsorbed per unit mass of *C. rupestris* at equilibrium (mg/g), C_e is the concentration of Cd(II) remaining in solution during adsorption equilibrium (mg/L), K_f is the Freundlich constant and indicative of the relative adsorption capacity of the adsorbent [(mg/g)(kg/mg)$^{1/n}$], and n is the Freundlich constant, indicating the intensity of adsorption (Farhan et al. 2013). LnQ_e is a function of $\ln C_e$, and n and K_f can be obtained from the slope and intercept.

Kinetics of adsorption of Cd by algae

The kinetic equations used to describe the metal ion biosorption process (Shen et al. 2017; Zhao et al. 2017; Zhang et al. 2017) are the following:

Pseudo-first-order adsorption rate equation,

$$\ln(Q_e - Q_t) = \ln Q_e^{-kt} \quad (3)$$

Pseudo-second-order adsorption rate equation,

$$t/Q_t = 1/k\, Q_e^2 + t/Q_e \quad (4)$$

Elovich equation,

$$Q_t = a + b \ln t \quad (5)$$

Double-constant equation,

$$\ln Q_t = a + b \ln t \quad (6)$$

where Q_t is the amount of Cd(II) adsorbed at t days (mg/kg), Q_e is the amount of Cd(II) adsorbed per unit mass of *C. rupestris* at equilibrium (mg/kg), K is apparent rate constant, a and b are defined as the rate constants of the Elovich and double-constant kinetics equations, and t was the time (days).

The data of this paper are expressed in Excel 2010 in the form of mean ± standard deviation (SD) with three repetitions. Pearson correlation coefficient and bilateral test method were used for correlation analysis; the conditions (normality and variance homogeneity) have been validated prior to correlation analysis. SPSS18.0 and Originpro8.5 software were used to analyze data and create diagrams.

Results and discussion

Biosorption effects and subcellular distribution of Cd in *C. rupestris*

The subcellular distribution of Cd is shown in Table 1, and Cd concentration in culture medium after different times is shown in Fig. 1, clearly indicating that *C. rupestris* accumulates Cd. The cumulative Cd capacity of *C. rupestris* ranges from 288.19 to 2735.3 mg/kg, and that bioconcentration factor (BCF) values reached up to 576. Brooks and Lee (1977) emphasized that the aboveground parts of a hyperaccumulator plant can accumulate up to 100 mg·kg^{-1} Cd. Thus, *C. rupestris* can be considered as a Cd hyperaccumulator plant (Cao et al. 2015a). Among all subcellular fractions, the cell wall exhibited the highest Cd concentration (Fig. 2). Cd concentrations in different subcellular fractions decreased in the following order: the cell wall and debris fraction (42.8–68.2%) > soluble fraction (22.1–38.4%) > organelle (11.6–30.5%). Moreover, Cd concentration markedly increased in different subcellular fractions with Cd supply (Fig. 2). When Cd concentration exceeded 5.0 mg/L, its proportion in cell organelles increased dramatically, indicating that high Cd concentration weakened the cell wall adsorption and is gradually

Table 1 Measured Cd contents in different parts of *C. rupestris* and BCF values

Cd stress level (mg/L)	Cd concentrations (mg/kg)				BCF
	Soluble fraction	Organelles	Cell wall	Total	
0.5	87.22 ± 2.29b	67.64 ± 1.05a	133.33 ± 0.83b	288.19	576
1.0	143.33 ± 1.82c	85.83 ± 1.10ab	280.00 ± 1.50bc	509.16	509
2.5	192.64 ± 4.79d	116.81 ± 4.19b	600.14 ± 8.91c	909.60	364
5.0	305.83 ± 1.50e	290.28 ± 3.18c	891.00 ± 61.02d	1487.1	297
7.5	395.14 ± 6.36f	414.75 ± 3.47d	1367.50 ± 1.10e	2177.4	290
10.0	518.08 ± 12.55 g	520.14 ± 2.14e	1697.08 ± 13.35f	2735.3	274

Note: The water content is 68.6–72.0%; the different letters on the same column indicate the different levels between the different treatments. BCF was bioconcentration factors of *C. rupestris*

transferred to cell organelles. These findings suggested that in *C. rupestris*, the cell wall plays a significant role in Cd retention at Cd concentration of ≤ 2.5 mg/L. By contrast, intracellular mechanisms mediate Cd retention at Cd concentration of > 2.5 mg/L Cd.

Previous studies showed that the cell wall and vacuoles play important roles in the tolerance, detoxification, and accumulation of heavy metals in plants (Zhang et al. 2011). The cell wall provides negatively charged sites on their multipleated surfaces that bind Cd ions and restrict Cd ion transport across the cytomembrane (Brune et al. 2008). Salt et al. (2002) reported that complexation with strong ligands, such as the thiol groups of phytochelatins and glutathione, also participates in detoxification. Consistent with the observations of Kramer et al. (2000), we found that under intensifying Cd stress, Cd is gradually transferred to organelles and soluble fraction components. So the *C. rupestris* has bioremediation potential of Cd.

Chemical forms of Cd

After the extraction of different chemical forms of Cd, the extracts exhibited the following order of Cd concentration: $F_{HAc} > F_{NaCl} > F_W > F_{HCl} > F_E$ (Fig. 3). The residual form of Cd in *C. rupestris* was lower than 0.1 mg/kg. Among these extracts, the 2% HAc extract had the largest proportion of Cd (43.2–56.0%) in the form of insoluble $CdHPO_4$ complexed with organic acids, $Cd(H_2PO_4)_2$, and other Cd-phosphate complexes (F_{HAC}), followed by 1 M NaCl extract containing pectate and protein-integrated Cd (F_{NaCl}), accounting for 30.8–43.2% Cd. The different chemical forms of Cd in *C. rupestris* increased in a concentration-dependent manner after Cd exposure.

Water-soluble inorganic and organic fractions of Cd (extracted with 80% ethanol and d-H_2O) have higher migration capacity and are more deleterious to plant cells than undissolved Cd phosphate (extracted with 2% HAc) and Cd oxalate (extracted with 0.6 M HCl) (Bai et al. 2014). In the present study, Cd was mainly present in the forms of insoluble $CdHPO_4$ complexed with organic acids in *C. rupestris*, $Cd(H_2PO_4)_2$, and other Cd-phosphate complexes (extracted with 2% HAc). These forms are less actively toxic than other forms, suggesting that their transport across cells is limited. At the Cd concentration of 2.5 mg/L, the proportion of low-activity and low-toxicity Cd (extracted with 2% HAC or

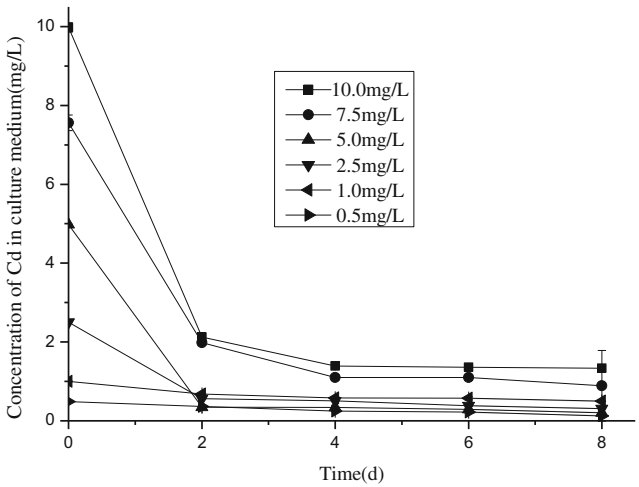

Fig. 1 Concentration of Cd in culture medium after different time

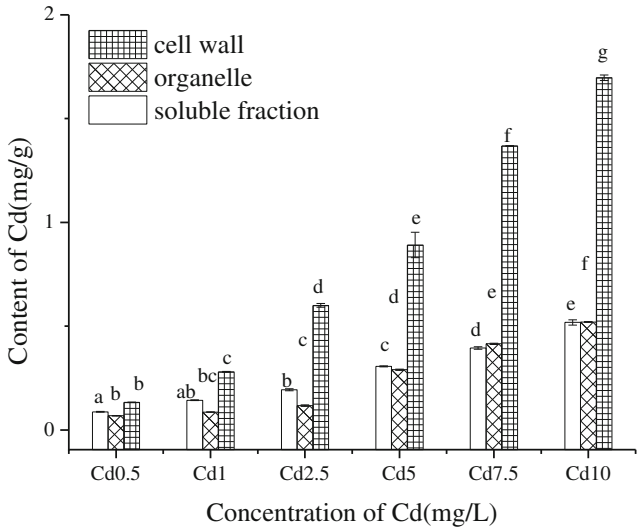

Fig. 2 The distribution of Cd in subcellular components

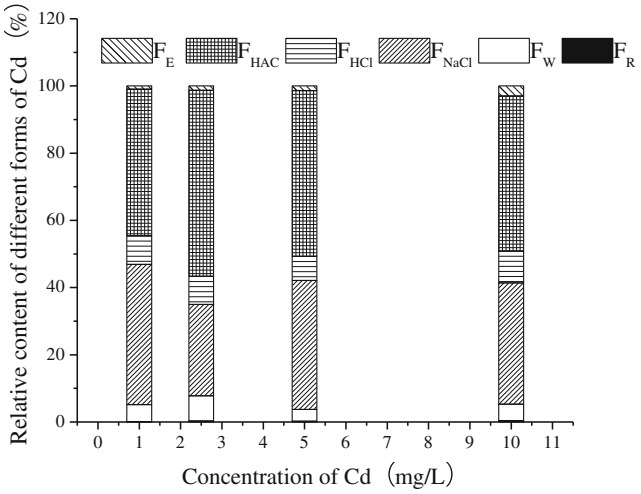

Fig. 3 Proportion of Cd in the storage forms in *C. rupestris*

0.6 M HCl) increased by 12.8% ($P < 0.05$). Bai et al. (2014) reported that *Viola tricolor* L. resists Cd toxicity by decreasing the proportion of soluble forms (extract by water and alcohol) of Cd. Similarly, the subcellular experiment revealed that at Cd concentration of < 5.0 mg/L, the Cd localization in the cell wall and soluble fraction attenuated organelle damage in *C. rupestris*. Other studies found similar results, and the chemical forms of Cd are related to its accumulation in the cell wall and in soluble fractions (Hernandez-Allica et al. 2006; Kupper et al. 2000). Krzesłowska (2011) reported that the complexation of Cd with mercapto and the side chains of protein or other organic compounds promote the complexation of Cd with pectic acid and protein. In *C. rupestris*, Cd enrichment in the cell walls decreases free intracellular Cd. This response ultimately attenuates Cd toxicity by increasing the amount of actively binding forms of Cd.

Kinetics of Cd in *C. rupestris*

Thermodynamic characteristics

The experimental results were analyzed using Langmuir and Freundlich adsorption models to describe the Cd biosorption characteristics of *C. rupestris* (Fig. 4). The R^2 value of the Freundlich isotherm model was 0.933, which was higher than that of the Langmuir isotherm model ($R^2 = 0.656$). This result indicated that the Freundlich model better fitted Cd biosorption by *C. rupestris* than the Langmuir model (Fig. 4a and b). These results are consistent with those obtained by Anastopoulos and Kyzas (2015), who stated that the Langmuir model fits well Cr(VI) adsorption by *Chlorella vulgaris*. Valuable information can also be observed from the model parameters (Areco et al. 2012). The Freundlich constant K_f indicates that the relative biosorption capacity of the biosorbent is related to bonding energy (Pillai et al. 2013). K_f = 0.638 reflects the low affinity and mobility of Cd to binding sites in *C. rupestris*. The Freundlich constant n indicates adsorption intensity. If the slope $1/n$ is less than 1, then a normal Freundlich isotherm is observed. Otherwise, cooperative adsorption can be observed (Fan et al. 2011). In the present study, the $1/n$ value (0.519) was less than 1, indicating that Cd adsorption by *C. rupestris* can be fitted by the normal Freundlich isotherm model. Most of the literatures suggested that the Freundlich model (Doshi et al. 2007; Mehta and Gaur

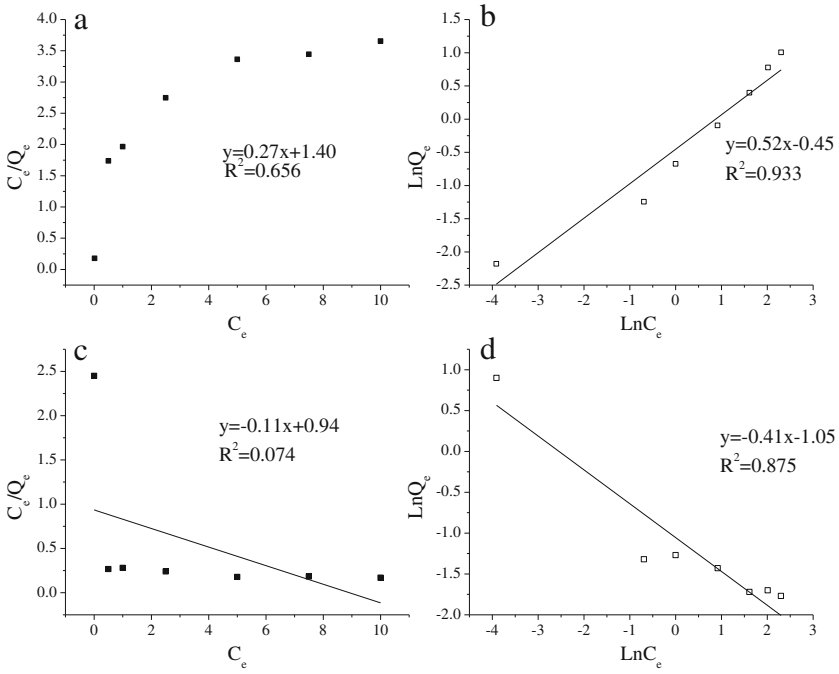

Fig. 4 Langmuir and Freundlich isotherm plot of Cd biosorption in *C. rupestris* (**a**), (**b**) as Langmuir and Freundlich isotherm plot of Cd biosorption in *C. rupestris* (**c**), (**d**) as Langmuir and Freundlich isotherm plot of Cd biosorption in cell wall of *C. rupestris*

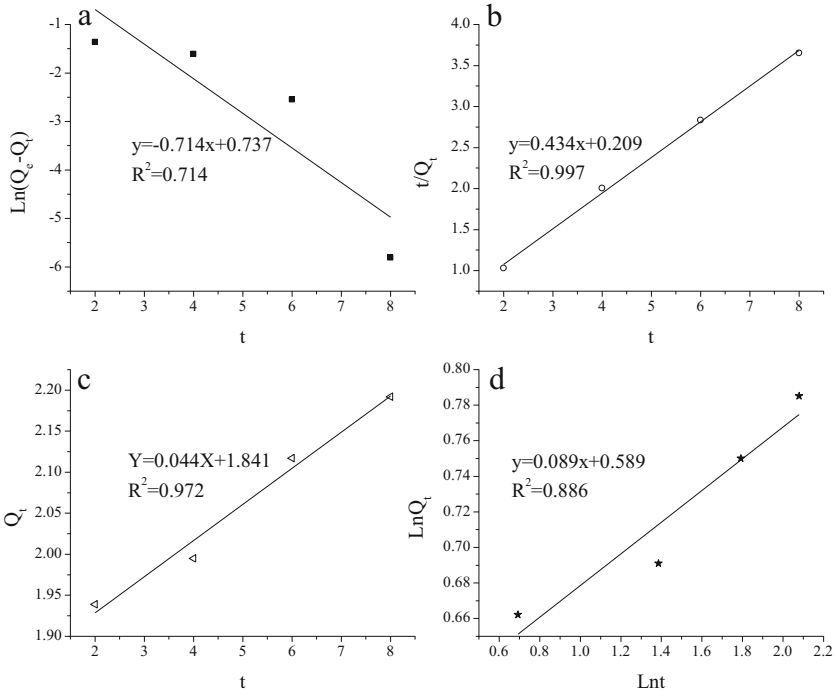

Fig. 5 Adsorption dynamics equation fitting results: **a** Pseudo-first-order adsorption rate equation, **b** Pseudo-second-order adsorption rate equation, **c** Elovich equation, **d** Double-constant equation

2001) fits well heavy metal absorption by living microalgae, which can remove heavy metals from water not only through cell-surface biosorption but also by cellular bioaccumulation. By contrast, the Langmuir isotherm model fits well the uptake process, which involves passive biosorption, of dead microbial cells or solid porous biosorbents (Huang et al. 2013; Ding et al. 2016). In the present study, the Freundlich isotherm model fitted well the Cd sorption by *C. rupestris* on the assumption that this process involves passive biosorption and initiative absorption.

The Langmuir and Freundlich adsorption models were used to analyze Cd biosorption on the cell walls of *C. rupestris* (Fig. 4c, d). R^2 of the Freundlich model was 0.875, indicating that the Freundlich model fitted well the biosorption data. However, the results of the Freundlich adsorption models better fitted the biosorption of the whole cell of *C. rupestris* than the cell wall only.

Kinetics characteristics of Cd adsorption

The kinetics data of Cd adsorption by *C. rupestris* at 25 °C were fitted with the pseudo-first-order and pseudo-second-order adsorption rate, Elovich, and double-constant rate equations (Fig. 5). The result indicated that the pseudo-second-order adsorption rate ($R^2 = 0.997$) and Elovich ($R^2 = 0.972$) equations have higher correlation coefficients than the other equations. The Elovich equation provides a description of the heterogeneous diffusion on the basis of the reaction rate and

Table 2 Correlation analysis of subcellular distribution and chemical forms of Cd in *C. rupestris*

r	Cell wall	Soluble fraction	Organelle	F_R	F_W	F_{Nacl}	F_{HCL}	F_{HAC}	F_E
Cell wall	1	− 0.501	0.644*	− 0.410	− 0.501	− 0.414	− 0.432	− 0.481	− 0.399
Soluble fraction		1	− 0.868**	0.931**	0.983**	0.989**	0.987**	0.986**	0.973**
Organelle			1	− 0.719**	− 0.786**	− 0.874**	− 0.807**	− 0.895**	− 0.734**
F_R				1	0.943**	0.926**	0.962**	0.915**	0.945**
F_W					1	0.959**	0.989**	0.957**	0.991**
F_{Nacl}						1	0.981**	0.982**	0.955**
F_{HCL}							1	0.975**	0.987**
F_{HAC}								1	0.946**
F_E									1

Note: *and ** mean data correlation between raw and column significantly at levels of 0.05 and 0.01

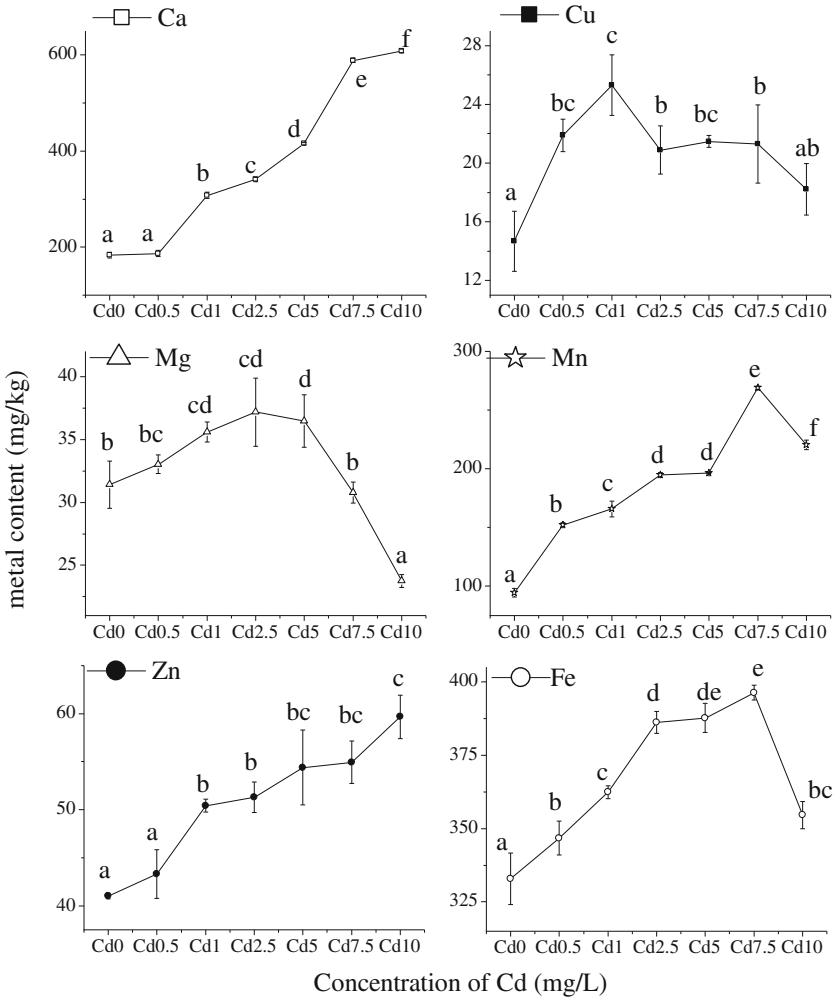

Fig. 6 Nutrient contents in *C. rupestris* affected by Cd

the diffusion factor (Zhao et al. 2017). The pseudo-second-order model assumes that the adsorption rate is controlled by the chemisorption mechanism (Kumar et al. 2016). Thus, complexation–biosorption properties and more than one mechanism would be involved in Cd biosorption by *C. rupestris*. Here, we found that Cd biosorption by *C. rupestris* involves active chemisorption and diffusion. This result was consistent with that reported by Talebi et al. (2013), who found that the second phase of biosorption by algal cells includes the uptake of heavy metal ions, wherein the first phase of biosorption consists of fast inactive adsorption on the cell surface.

Correlation analysis between the subcellular distribution and chemical forms of Cd in *C. rupestris*

Correlation analysis revealed that in *C. rupestris*, the chemical forms of Cd present in soluble fractions and organelles are strictly correlated with Cd concentration ($P < 0.01$) (Table 2). The content of each chemical form of Cd in soluble fractions increased with Cd concentration and decreased in cell organelles with Cd concentration. Under intensifying Cd stress levels, Cd was gradually transferred to organelles and vacuolar components, and vacuolar compartmentalization transformed the chemical forms of Cd into low-toxicity forms to defend against toxicity. This response is consistent with the conclusion presented in Cao et al. (2018).

Effects of Cd on metal homeostasis in *C. rupestris*

Cd stress caused mineral imbalance and disrupted the internal stability of mineral nutrition in *C. rupestris*. Cd treatment promoted the uptake of Ca and Zn (Fig. 6, $R_{Ca}^2 = 0.9194$, $P < 0.05$; $R_{Zn}^2 = 0.899$, $P < 0.05$). The absorption of Cu, Fe, Mn, and Mg was promoted by Cd concentrations, especially at Cd concentrations lower than 7.5 mg/L, but Mg uptake was inhibited by 10 mg/L Cd. The Mg concentration was lower than 25 mg/kg (Fig. 6). Cd can indirectly affect the growth and metabolism of plants by affecting the absorption of mineral nutrients, and nutrition status can greatly influence the

capability of plants to accumulate heavy metals (Sarwar et al. 2010; Singh et al. 2010; Cao et al. 2018). Cd uptake and toxicity were observed in green alga (*Chlamydomonas reinhardtii*) after long-term exposure (60 h) to a range of environmentally realistic free Zn, Co, Fe, Mn, Ca, and Cu (Lavoie et al. 2012). Ca plays an important role in maintaining the stability of cell wall structure and thus enhances plant resistance (Cao et al. 2015b). Furthermore, enhancing cell wall stability by increasing Ca content is related to Cd enrichment in the cell wall. Zn is involved in plant transpiration and participates in auxin formation, photosynthesis, and protein synthesis. Increased Zn uptake may also be related to the coaccumulation relationship between Zn and Ca (Sarret et al. 2006). The decrease in Mg content inhibited the photosynthesis of *C. rupestris* because Mg is an important component of chlorophyll. Siedlecka and Krupa (1999) reported that the replacement of Mg, which is the central atom of chlorophyll, with Hg, Cu, Cd, or other heavy metal ions, disrupts photosynthesis. Importantly, Ren and Sheng (2017) proposed that the homeostatic balance between Ca^{2+} and Mg^{2+} is a critical feature of plant mineral nutrition for optimal growth and development under changes in soil nutrient status.

Conclusion

Our study demonstrated that *C. rupestris* could accumulate Cd. Cd mainly accumulates in the cell walls and soluble fractions in *C. rupestris*. Under Cd stress, a large quantity of Cd ions exists in *C. rupestris* in the forms of insoluble $CdHPO_4$ complexed with organic acids, $Cd(H_2PO_4)_2$, and other Cd-phosphate complexes. Cd complexation–biosorption involves passive biosorption and initiative absorption. Cell wall adsorption has an important role in the Cd adsorption ability and process of *C. rupestris*. Cell wall sequestration, vacuolar compartmentalization, and chemical morphological transformation are likely essential mechanisms for Cd detoxification and biosorption by *C. rupestris*. The adsorption data were well fitted by the Freundlich model ($R^2 = 0.933$) and could be described by the pseudo-second-order reaction rate ($R^2 = 0.997$) and Elovich ($R^2 = 0.972$) equations. Related parameters indicated that Cd adsorption by *C. rupestris* is a heterogeneous diffusion. Cd promoted Ca and Zn uptake by *C. rupestris*. Cu, Fe, Mn, and Mg adsorption was promoted by low Cd concentrations and inhibited by high Cd concentrations. This study suggests that *C. rupestris* has bioremediation potential of Cd.

Funding information This work was under the financial aid of the Natural Science Foundation of China (41877418), Nature Fund of Anhui Province of China (1808085MD100), and the Key S&T Special Projects of Anhui Province of China (17030701053), and funding for this study was also provided by the Natural Students' Innovation and Entrepreneurship Training Program (201710364058).

References

Anastopoulos I, Kyzas GZ (2015) Progress in batch biosorption of heavy metals onto algae. J Mol Liq 209:77–86

Areco MM, Hanela S, Duran J, Afonso MS (2012) Biosorption of Cu(II), Zn(II), Cd(II) and Pb(II) by dead biomasses of green alga *Ulva lactuca* and the development of a sustainable matrix for adsorption implementation. J Hazard Mater 213–214:123–132

ATDR (2012) Toxicological profile for cadmium, Agency for Toxic Substances and Disease Registry. Public Health Services, US Department of Health and Human Services. J Mol Liq 209:77–86

Bai X, Chen YH, Geng K et al (2014) Accumulation, subcellular distribution and chemical forms of cadmium in *Viola tricolor L*. China. J Acta Scientiae Circumstantiae 34(6):1600–1605

Brooks RR, Lee J, Reeves RD, Jaffre T (1977) Detection of nickeliferous rocks by analysis of herbarium specimens of indicator plants. J Geochem Explor 7:49–77

Brune A, Urbach W, Detz KJ (2008) Compartmentation and transport of zinc in barley primary leaves as basic mechanism involved in zinc tolerance. Plant Cell Environ 17:153–162

Cao DJ, Shi XD, Li H, Xie PP, Zhang HM, Deng JW, Liang YG (2015a) Effects of lead on tolerance, bioaccumulation, and antioxidative defense system of green algae, *Cladophora*. Ecotoxicol Environ Saf 112:231–237

Cao DJ, Xie PP, Deng JW, Zhang HM, Ma RX, Liu C, Liu RJ, Liang YG, Li H, Shi XD (2015b) Effects of Cu^{2+} and Zn^{2+} on growth and physiological characteristics of green algae, *Cladophora*. Environ Sci Pollut Res 22:16535–16541

Cao DJ, Yang X, Geng G, Wan XC, Ma RX, Zhang Q, Liang YG (2018) Absorption and subcellular distribution of cadmium in tea plant (*Camellia sinensis* cv. "Shuchazao"). Environ Sci Pollut Res 25(16):15357–15367

Chakravarty R, Banerjee PC (2012) Mechanism of cadmium binding on the cell wall of an acidophilic bacterium. Bioresour Technol 108: 176–183

Ding Y, Liu Y, Liu S, Li Z, Tan X, Huang X, Zeng G, Zhou Y, Zheng B, Cai X (2016) Competitive removal of Cd(II) and Pb(II) by biochars produced from water hyacinths: performance and mechanism. RSC Adv 6:5223–5232

Doshi H, Ray A, Kothari IL (2007) Bioremediation potential of live and dead Spirulina: spectroscopic, kinetics and SEM studies. Biotechnol Bioeng 96:1051–1063

Fan JL, Zhang J, Zhang CL et al (2011) Adsorption of 2,4,6-trichlorophenol from aqueous solution onto activated carbon derived from loosestrife. Desalination 267:139–146

Farhan AM, Al-Dujaili AH, Awwad AM (2013) Equilibrium and kinetic studies of cadmium(II) and lead(II) ions biosorption onto *Ficus carcia leaves*. Int J Ind Chem 4:24

Fu XP, Dou CM, Chen YX, Chen XC, Shi JY, Yu MG, Xu J (2011) Subcellular distribution and chemical forms of cadmium in Phytolacca americana L. J Hazard Mater 186:103–107

Hassler CS, Slaveykova VI, Wilkinson KJ (2004) Discrimination between intra- and extracellular metals using chemical extractions. Limnol Oceanogr Methods 2:237–247

Hernandez-Allica J, Garbisu C, Becerril JM et al (2006) Synthesis of low molecular weight thiols in response to Cd exposure in *Thlaspi caerulescens*. Plant Cell Environ 29(7):1422–1429

Hou M, Hu CJ, Xiong L, Lu C (2013) Tissue accumulation and subcellular distribution of vanadium in Brassica juncea and Brassica chinensis. Microchem J 110:575–578

Huang F, Dang Z, Guo CL, Lu GN, Gu RR, Liu HJ, Zhang H (2013) Biosorption of Cd(II) by live and dead cells of *Bacillus cereus RC-1* isolated from cadmium-contaminated soil. Colloids Surf B 107:11–18

Islam MS, Saito T, Kurasaki M (2015) Phytofiltration of arsenic and cadmium by using an aquatic plant, *Micranthemum umbrosum*: phytotoxicity, uptake kinetics, and mechanism. Ecotoxicol Environ Saf 112:193–200

Kramer U, Pickering IJ, Prince RC et al (2000) Subcellular localization and speciation of nickel in hyperaccumulator and non-accumulator *Thlaspi* species. Physiol Plant 122:1343–1353

Krzesłowska M (2011) The cell wall in plant cell response to trace metals: polysaccharide remodeling and its role in defense strategy. Acta Physiol Plant 33:35–51

Kumar D, Pandey LK, Gaur JP (2016) Metal sorption by algal biomass: from batch to continuous system. Algal Res 18:95–109

Kupper H, Lombi E, Zhao FJ et al (2000) Cellular compartmentation of cadmium and zinc in relation to other elements in the hyperaccumulator *Arabidopsis halleri*. Planta 212(1):75–84

Lavoie M, Le Faucheur S, Fortin C, Campbell PGC (2009a) Cadmium detoxification strategies in two phytoplankton species: metal binding by newly synthesized thiolated peptides and metal sequestration in granules. Aquat Toxicol 92(2):65–75

Lavoie M, Bernier J, Fortin C, Campbell PGC (2009b) Cell homogenization and subcellular fractionation in two phytoplanktonic algae: implications for the assessment of metal subcellular distributions. Limnol Oceanogr Methods 7(4):277–286

Lavoie M, Fortin C, Campbell PGC (2012) Influence of essential elements on cadmium uptake and toxicity in a unicellular green alga: the protective effect of trace zinc and cobalt concentrations. Environ Toxicol Chem 31(7):1445–1452

Li H, Luo N, Zhang LJ, Zhao HM (2016) Do arbuscular mycorrhizal fungi affect cadmium uptake kinetics, subcellular distribution and chemical forms in rice? Sci Total Environ 571:1183–1190

Li XJ, Zheng XQ, Zheng SA (2017) Accumulation and sensitivity distribution of cadmium in leafy vegetables. J Res Environ Sci 30(5): 720–727

Lwalaba JLW, Zvobgo G, Mwamba M, Ahmed IM, Mukobo RPM, Zhang G (2017) Subcellular distribution and chemical forms of Co^{2+} in three barley genotypes under different Co^{2+} levels. Acta Physiol Plant 39:102

Ma J, Cai H, He C, Zhang W, Wang L (2015) A hemicellulose-bound form of silicon inhibits cadmium ion uptake in rice (*Oryza sativa*) cells. New Phytol 206:1063–1074

Mehta SK, Gaur JP (2001) Removal of Ni and Cu from single and binary metal solutions by free and immobilized Chlorella vulgaris. Eur J Protistol 271:261–271

Meyer CL, Juraniec M, Huguet S, Chaves-Rodriguez E, Salis P, Goormaghtigh E, Verbruggen N (2015) Intraspecific variability of cadmium tolerance and accumulation, and cadmium-induced cell wall modifications in the metal hyperaccumulator Arabidopsis halleri. J Exp Bot 66:3215–3217

Mwamba TM, Li L, Gill RA et al (2016) Differential subcellular distribution and chemical forms of cadmium and copper in *Brassica napus*. Ecotoxicol Environ Saf 134:239–249

Pillai SS, Mullassery MD, Fernandez NB, Girija N, Geetha P, Koshy M (2013) Biosorption of Cr(VI) from aqueous solution by chemically modified potato starch: equilibrium and kinetic studies. Ecotoxicol Environ Saf 92:199–205

Qiu Q, Wang Y, Yang Z, Yuan J (2011) Effects of phosphorus supplied in soil on subcellular distribution and chemical forms of cadmium in two Chinese flowering cabbage (*Brassica parachinensis* L) cultivars differing in cadmium accumulation. Food Chem Toxicol 49:2260–2267

Ren JT, Sheng L (2017) Regulation of calcium and magnesium homeostasis in plants: from transporters to signaling network. Curr Opin Plant Biol 39:97–105

Salt DE, Prince RC, Pickering IJ (2002) Chemical speciation of accumulated metals in plants: evidence from X-ray absorption spectroscopy. Microchem J 71:255–259

Sarret G, Harada E, Choi YE, Isaure MP, Geoffroy N, Fakra S, Marcus MA, Birschwilks M, Clemens S, Manceau A (2006) Trichomes of tobacco excrete zinc as zinc-substituted calcium carbonate and other zinc-containing compounds. Plant Physiol 141(3):1021–1034

Sarwar N, Malhi SS, Zia MH, Naeem A, Bibi S, Farid G (2010) Role of mineral nutrition in minimizing cadmium accumulation by plants. J Sci Food Agric 90:925–937

Shen Y, Li H, Zhu WZ, Ho SH, Yuan WQ, Chen JF, Xie YP (2017) Microalgal-biochar immobilized complex: a novel efficient biosorbent for cadmium removal from aqueous solution. Bioresour Technol 244:1031–1038

Siedlecka A, Krupa Z (1999) Cd/Fe interaction in higher plants: its consequences for the photosynthetic apparatus. Photosynthetica 36: 321–331

Singh A, Agrawal M, Marshall FM (2010) The role of organic vs. inorganic fertilizers in reducing phytoavailability of heavy metals in a wastewater-irrigated area. Ecol Eng 36:1733–1740

Talebi AF, Tabatabaei M, Mohtashami SK, Tohidfar M, Moradi F (2013) Comparative salt stress study on intracellular ion concentration in marine and salt-adapted freshwater strains of microalgae. Not Sci Biol 5(3):309–315

Wang L, Chen X, Wang H, Zhang Y, Tang Q, Li J (2017) Chlorella vulgaris cultivation in sludge extracts from 2,4,6-TCP wastewater treatment for toxicity removal and utilization. J Environ Manag 187: 146–153

Xie PP, Deng JW, Zhang HM, Ma YH, Cao DJ, Ma RX, Liu RJ, Liu C, Liang YG (2015) Effects of cadmium on bioaccumulation and biochemical stress response in rice (*Oryza sativa* L). Ecotoxicol Environ Saf 122:392–398

Yang MQ, Li HY (2015) Study on biosorption of heavy metals by algae. Anhui Agricultural Sciences 43(28):257–259

Zeraatkar AK, Ahmadzadeh H, Talebi AF, Moheimanic NR, McHenryd MP (2016) Potential use of algae for heavy metal bioremediation, a critical review. J Environ Manag 181:817–831

Zhang J, Tian SK, Lu LL et al (2011) Lead tolerance and cellular distribution in Elsholtzia splendens using synchrotron radiation micro-X-ray fluorescence. J Hazard Mater 197:264–271

Zhang HJ, Gao YT, Xiong HB (2017) Removal of heavy metals from polluted soil using the citric acid fermentation broth: a promising washing agent. Environ Sci Pollut Res 24:9506–9514

Zhao YF, Wu JF, Shang DR, Ning JS, Zhai YX, Sheng XF, Ding HY (2015) Subcellular distribution and chemical forms of cadmium in the edible seaweed, Porphyra yezoensis. Food Chem 168:48–54

Zhao S, Huang GH, Mu S, An CJ, Chen XJ (2017) Immobilization of phenanthrene onto gemini surfactant modified sepiolite at solid/aqueous interface: equilibrium, thermodynamic and kinetic studies. Sci Total Environ 598:619–627

Zhou XD, Li CY, Gao PX, Jiang XC, Zhao ZY, Han WS (2017) Adsorption of Cd^{2+} in water by living microalgae. Microbiol China 44(5):1182–1188